Sustainable Steel Decarburization by Oxide Addition

Othman N. Alzeghaibi*, Charles C. Sorrell, and Veena H. Sahajwalla

School of Materials Science and Engineering, University of New South Wales, Sydney NSW   2052, Australia

Abstract: The decarburization of liquid steel has been investigated using a new approach involving oxide addition and inert atmosphere instead of the conventional method of blowing oxygen and/or applying vacuum/stirring.   The method included preliminary free energy calculations to predict oxide decomposition and CO formation at steelmaking temperature.   The experimental method included mixing 1 wt% Fe_2O_3, Fe_3O_4, or NiO to high-purity iron powder containing ≤0.05 wt% C and ≤0.33 O; rotary mixing for ~8 h, pelletizing at 650 kPa; and instantaneous heating/melting at 1600°C for 20 min under flowing Ar (1 L/min).   LECO® analysis, IR gas analysis, and video imaging confirmed that CO formation and evacuation were responsible for decarburization to ultra-low C concentrations.   The lowest final C level achieved of 13.6 ppm resulted from Fe_2O_3 addition.   The data confirm that free energy calculations can be used to identify suitable oxide additions.   The present work also demonstrates that decarburization to levels sufficient for ultra-low carbon steels (≤50 ppm) can be achieved by a four-stage process: (a) decomposition of the oxide, (b) consequent addition of alloying element and oxygen to the steel, (c) resultant decarburization by CO formation and evacuation, and (d) associated convective homogenization from the effects of the gas.

Keywords: Oxide addition, Decarburization, Liquid steel, Ultra-low carbon steel

1. Introduction

It is well known that steel is an alloy of iron containing relatively low levels of carbon (*viz.*, 0.2 wt% maximum).   A variety of steelmaking processes is used to achieve targeted chemistries at high temperatures (*viz.*, ~1600°C) and these vary on a steel grade-to-grade basis, where the amounts of each alloying element and carbon result in properties specific to the final product for different applications. These processes include deoxidation, decarburization, dephosphorization, desulphurization, hydrogen removal, and nitrogen removal.

Liquid steel for casting of normal grades of steel (high-, medium-, and low-carbon; ≥0.01 wt% carbon) is produced by the two routes of (a) direct reduction (DR) for electric arc furnace (EAF) steelmaking and (b) blast furnace (BF) technology for basic oxygen furnace (BOF) steelmaking.   In both processes, the iron ore is reduced, melted, and poured into a ladle.   The chemistry of the liquid steel and its temperature in the ladle are adjusted and homogenized, followed by casting.

However, the further removal of carbon (<0.01 wt%) slows owing to the approach of equilibrium at these lower carbon levels [1].   Also, additional treatments by the processes mentioned above are required for special steel grades with lower levels of other elements.   These equilibrium and kinetics issues typically are addressed by the use of top oxygen blowing (for carbon removal) and/or vacuum/stirring (for removal of all residuals).

These processes can produce ultra-low carbon steels (≤0.005 wt%) and they are used as the bases for a range of grades, including automotive, electric, deep drawing quality (DDQ), extra-deep drawing quality (EDDQ), interstitial-free (IF), and ultra-low carbon (ULC) steels.

The present proof-of-concept work involves a new approach combining simultaneous alloying, decarburization, and homogenization through the addition of oxides to liquid steel under inert atmosphere. The selection of oxide additions was based on the highly negative free energies for the general reaction:

$$Oxide + Carbon \rightarrow Metal + Carbon\ Monoxide \tag{1}$$
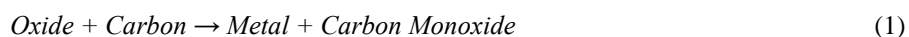
2. Experimental Procedure

The base raw material, a high-purity iron powder, marketed under the name *carbonyl iron*, was obtained from BASF (Germany). Its relevant characteristics, reported by the manufacturer, are given in Table 1.

Table 1   Characteristics of *Carbonyl Iron*

Chemical Analysis						
Unit	Weight % (wt%)			Parts per Million (ppm)		
Element	Fe	C	N	O	Cr	Ni	Mo
Amount	≥99.5	≤0.05	≤0.01	≤0.33	≤50	≤50	≤50
Particle Size Distribution						
D_{10} (μm)	4.4					
D_{50} (μm)	9.5					
D_{90} (μm)	33					

LECO® analysis of the carbonyl iron powder revealed that the actual carbon and oxygen levels were 0.007 wt% and 0.20 wt%, respectively.

The oxides Fe_2O_3, Fe_3O_4, and NiO were selected for addition owing to the negative free energies for oxide decomposition and CO formation. A 10 g batch of carbonyl iron was weighed, 0.100 g of an oxide was added (1 wt%), the blend was placed in a glass container, it was mixed by rotation for 8 h, the mixture was placed in a 15 mm diameter hardened steel die, and it was uniaxially pressed at 650 kPa for 20 s. A control sample without oxide addition also was prepared.

For stoichiometric reaction between the oxygen liberated from the oxide and the initial carbon, the required amount of the former is 0.000932 g. Hence, the calculated levels of oxide necessary for addition were 0.00931 g, 0.01349 g, and 0.00435 g for Fe_2O_3, Fe_3O_4, and NiO, respectively. Since 0.1 g (1 wt%) of oxide was added, it is clear that the additional levels used were substantially greater than those required for stoichiometric reaction to form CO. These levels were selected essentially arbitrarily since the present work was designed as an exploratory investigation to probe the feasibility of the approach.

The appearances of the powder and the pressed sample are shown in Figure 1.

Fig. 1 Carbonyl iron powder and pressed sample

The decarburization procedure used a horizontal tube furnace (50 mm diameter) with controlled atmosphere capability, associated infrared (IR) gas sensor, and external charge-coupled device (CCD) camera. A schematic cross-section of the experimental set-up is shown in Figure 2.
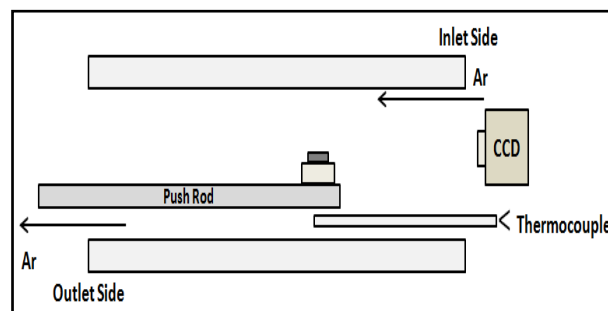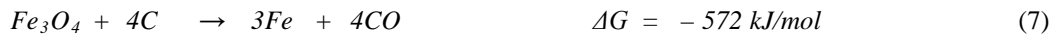

Fig. 2 Schematic of experimental set-up

The procedures consisted of the following stages:

- The furnace was sealed and the atmosphere was purged from the inlet side with flowing Ar (1 L/min) for ~30-60 min until the IR sensor indicated that the CO and CO_2 concentrations had stabilized.
- The pellet was placed in a LECO® crucible of Al_2O_3-ZrO_2-SiO_2 (AZS).
- The furnace port on the outlet side was opened momentarily and the crucible was loaded into the furnace tube. The IR sensor indicated that no oxygen contamination occurred during this stage since the CO and CO_2 concentrations remained constant.
- The CCD imaging camera was activated.
- The crucible was pushed manually into the hot zone at 1600°C over a period of a few seconds using a sliding graphite push rod, which maintained a furnace seal with an O-ring.
- The crucible remained in the hot zone of the furnace for ~20 min. The IR sensor indicated that the reaction processes had ceased by this time point.
- The crucible was pulled out of the hot zone and allowed to cool over ~30 min until it reached ~500°C.
- The furnace port was opened, the crucible was removed, and it was allowed to cool to room temperature.

3. Results

(1) *Thermodynamics:*   The free energies of reaction at 1600°C were calculated according to a range of available data [2-8].   The free energies of the reactions MO + C → M + CO were highly negative and so were expected to proceed readily.

The primary reactions and their free energies are as follows:

$$C \quad + \; O \quad \rightarrow \quad CO \qquad\qquad\qquad \Delta G \; = \; - \;\; 94 \; kJ/mol \qquad (2)$$

$$O \quad + \; O \quad \rightarrow \quad O_2 \qquad\qquad\qquad \Delta G \; = \; - \; 444 \; kJ/mol \qquad (3)$$

$$C \quad + \; \tfrac{1}{2}O_2 \quad \rightarrow \quad CO \qquad\qquad\qquad \Delta G \; = \; - \; 275 \; kJ/mol \qquad (4)$$

$$FeO \; + \; C \quad \rightarrow \quad Fe \; + \; CO \qquad\qquad \Delta G \; = \; - \; 127 \; kJ/mol \qquad (5)$$

$$Fe_2O_3 + \; 3C \quad \rightarrow \quad 2Fe \; + \; 3CO \qquad \Delta G \; = \; - \; 478 \; kJ/mol \qquad (6)$$

$$Fe_3O_4 + \; 4C \quad \rightarrow \quad 3Fe \; + \; 4CO \qquad \Delta G \; = \; - \; 572 \; kJ/mol \qquad (7)$$

$$NiO \; + \; C \quad \rightarrow \quad Ni \; + \; CO \qquad\qquad \Delta G \; = \; - \; 200 \; kJ/mol \qquad (8)$$

(2) *Carbon Removal:*   The removal of carbon in the form of CO was detected using the IR sensor.   Any CO_2 that may have formed remained below the level of detection both before and during the experiments. The results for the control and the three samples with oxide addition are shown in Figure 3.
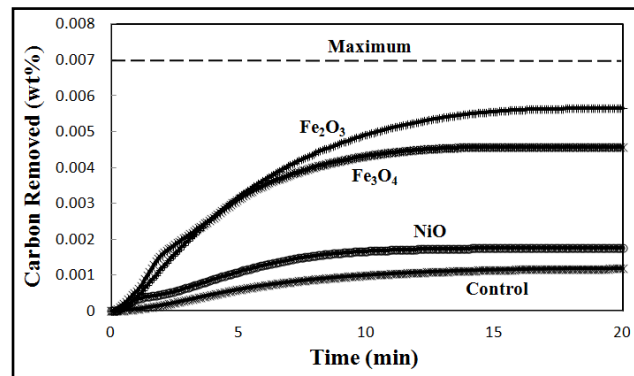

Fig. 3   Carbon removal at 1600°C

(3) *Gas Evolution:*   Qualitative assessment of the CO evacuation from the liquid steel was done using the CCD imaging camera.   Proof of the presence of gas evolution from within the sample was confirmed by the observation of surface profile features consistent with the formation of pore cavities.   Proof of the cessation of gas evolution was confirmed by the simultaneous disappearance of these surface profile features (final stage not shown) in addition to the volume reduction and stabilization of the sample.   These data are shown in Figure 4.
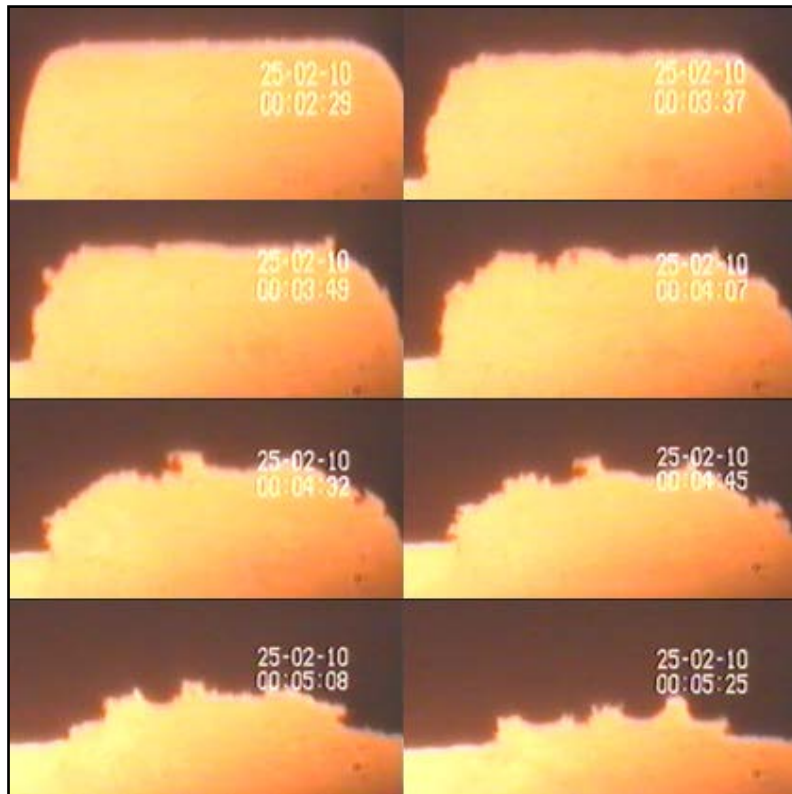
Fig. 4　CCD images of sample containing Fe_3O_4 over 5 min at 1600°C

4. Discussion

The basic thermodynamic analyses confirm that decarburization by oxide addition is possible [10]. These analyses also highlight the probable importance of oxygen present in or on the powder or added extrinsically.

The carbon removal data, shown in Figure 3, demonstrate that the addition of an iron oxide substantially improves both the amount and rate of carbon reduction in the samples through the associated process of CO formation. NiO was considerably less effective.

Table 2 summarizes the measured carbon levels achieved during decarburization. These data show that there is limited decarburization of the control sample, decreasing the carbon level from 70.0 ppm to 58.2 ppm. In contrast, when one of these oxides is added, the carbon levels decreased to the range 13.6-52.5 ppm.

Table 2　Steel decarburization data after 20 min at 1600°C

Sample	Carbon Removed		Final Carbon	
	Wt%	ppm	Wt%	ppm
Powder	0	0	0.00700	70.0
Control	0.00118	11.8	0.00582	58.2
1 wt% Fe_2O_3	0.00564	56.4	0.00136	13.6
1 wt% Fe_3O_4	0.00458	45.8	0.00242	24.2
1 wt% NiO	0.00175	17.5	0.00525	52.5

These data may be placed in context by contrasting the total amounts of oxygen deriving from the added oxides plus that present initially in the powder (0.20 wt%) with those of the final carbon levels.   Table 3 and Figure 5 summarize these values.

Table 3   Comparison of oxygen levels in liquid steel and final carbon levels

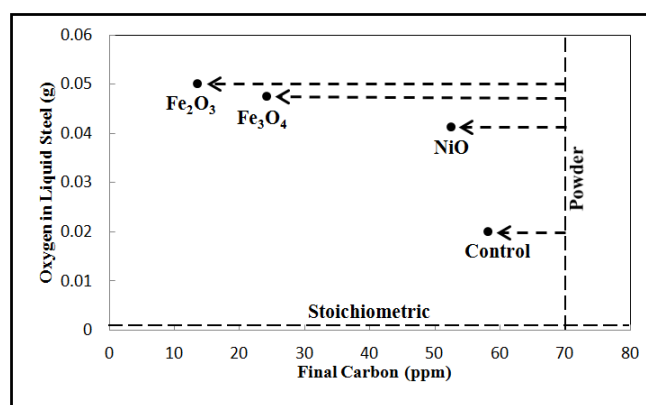| Sample	Oxygen in Liquid Steel (g)			Final Carbon
	Stoichiometric	From Oxide	Total Present	
Control	0.000932	0	0.0200	58.2
1 wt% Fe_2O_3	0.000932	0.0301	0.0501	13.6
1 wt% Fe_3O_4	0.000932	0.0276	0.0476	24.2
1 wt% NiO	0.000932	0.0214	0.0414	52.5

Fig. 5   Final carbon level as a function of oxygen level in liquid steel

The preceding data illustrate graphically the following features:

- All of the samples with oxide additions have substantially more oxygen than is required for stoichiometric reaction to form CO.
- The oxide samples show a greater amount of decarburization relative to the control.
- For the former samples, the effectiveness of decarburization is directly proportional to the amount of oxygen in excess of stoichiometric (*viz.*, the Total Present in Table 3).
- The control is closest to the stoichiometric oxygen requirement.
- This sample shows the least amount of decarburization.

It is notable that, while the trend in the effect of oxygen is as expected from stoichiometry considerations in terms of both the relation between (a) the control and the samples with oxide additions and (b) the three samples with oxide additions, the previous study by the authors [10] shows the converse effect.   In that case, the trend in the effect of oxygen was reversed from that expected.   These results confirm that it is unlikely that the presence of a stoichiometric ratio of oxide to achieve reaction with C to form CO is the only factor to consider.   Similarly, other relevant considerations include the effects of (a) the dissolved alloying element, (b) the dissolved excess oxygen, (c) the potential formation of intermetallic and/or oxide precipitates, (d) the non-alloying effect of iron, (e) the spontaneous release of oxygen from both iron oxides above ~1400°C [11], and (f) the probable differences in reactivity with

dissolved carbon between chemical (dissolved) oxygen and physical (exsolved) oxygen.   In particular, the first two factors could affect the viscosity and/or the surface tension of the liquid steel, both of which would impact on the rate of bubble evacuation.   However, these factors are difficult to assess without further information.   Regardless, the achievement of steady-state conditions after ~15 min, as shown in Figure 3, indicates that bubble evacuation was complete in all cases but the rate at which this occurred varied.

The CCD images, shown in Figure 4, demonstrate the onset of gas evolution, its agitating effect on the surface smoothness, and the termination of the process.   The surface roughness formed upon collapse of the pores established when CO and/or O_2 bubbles reached the surface.   The reduction in the sample volume is consistent with the elimination of all bubbles from inside the sample.   This also tends to confirm the preceding comment concerning the completion of bubble evacuation.

It is likely that convective mixing, which would be facilitated by the CO and/or O_2 bubble formation and transit to the surface, facilitated the effectiveness of the decarburization.   Also, there may be a beneficial effect of excess oxygen from the addition and the oxygen released from the iron oxides when it is evacuated in the form of oxygen bubbles, which would increase the amount of convective mixing.

5. Conclusions

The present work demonstrates that adding oxygen in the form of a solid oxide to liquid steel can be effective in achieving substantial levels of decarburization in a period of ~15 min in flowing Ar.   This may be contrasted with the requirements of top oxygen blowing, vacuum degassing, and stirring, which require similar or longer times to reach equivalent final carbon levels but with the requirement of more elaborate facilities and processes [9].

A second related advantage is the improved homogenization that this approach entails.   That is, top oxygen blowing is directional over a limited area [9] whereas the present work involves more homogeneous compositional and thermal distributions owing to the convective mixing.

Further, even though these preliminary results were not optimised and used an arbitrary additional level of 1 wt% oxide, in each case, a carbon level equivalent to or less than that of ultra-low carbon steels (<50 ppm) was obtained. Thus, it is possible that further refinement of the type and amount of oxide addition could reduce the residual carbon level to that achieved in more typical ultra-low carbon steels, which is ~20 ppm.

Such low levels of residual carbon may be facilitated through the enhanced convective mixing.   That is, the amount of CO and/or O_2 evolution is likely to be increased by optimizing the oxide:carbon ratio, although it is unknown if this ratio is stoichiometric.   These issues may be dominated by the effects of the oxide additions on the viscosity and/or surface tension of the liquid steel, both of which would affect the kinetics of the process of bubble evacuation. However, since two of the three samples did not contain an alloying metal and these showed the highest levels of decarburization, these observations and the data for other oxide additions [10] suggest that the dominant effect may be that of the alloying metal on the viscosity and/or surface tension.

In the present work, the effect of the type and amount of alloying element on the steel properties were not considered. It is clear that the present approach to decarburization also may involve an improved method of alloy addition. For example, it may be possible to eliminate the requirement of the addition of ferromanganese, which is expensive, by substitution with inexpensive MnO, Mn_2O_3, Mn_3O_4, or MnO_2. The fine particle sizes of the oxide powders (compared to coarser ferromanganese) and the convective mixing are likely to improve the rate of chemical mixing and the ultimate homogeneity of the alloying element.

For the preceding reasons, it can be concluded that that the present work indicates that decarburization by oxide addition offers a number of advantages in cost, raw materials usage, and productivity. It also offers the interesting possibility that the addition of an iron oxide, which may result in enhanced thermal and chemical homogenization and associated oxygen evacuation, may reduce or eliminate the need for deoxidation. In these senses, the process may be viewed in terms of improved sustainability of the steelmaking process.

Acknowledgements

References

[1] M.A. Makarov, A.A. Aleksandrov, and V.Ya. Dashevskii. Deep decarburization of iron-based melts. *Russ. Metall. (Metally)*, 2007, 2007, p91-97.

[2] Y. Kawai and M. Katsumi. Steelmaking Data Sourcebook. Editors: The Japan Society for the Promotion of Science – The 19th Committee on Steelmaking, Gordon & Breach, New York, NY, 1988.

[3] T. Mori, E. Ichise, and A. Moro-Oka. Steelmaking Data Sourcebook. Editors: The Japan Society for the Promotion of Science – The 19th Committee on Steelmaking, Gordon & Breach, New York, NY, 1988.

[4] C. Bodsworth and H.B. Bell. Physical Chemistry of Iron and Steel Manufacture, 2nd ed., Longman Group Limited, London, UK, 1972.

[5] *FactSage™ 6.2*, ThermFact Inc. and GTT-Technologies, 2010.

[6] E. Turkdogan. Physical Chemistry of High Temperature Technology, Academic Press, New York, NY, 1980.

[7] E. Turkdogan. Synchronising free energy data on reactions in liquid Fe-Mn-O and solid Mn-S-O systems. *Ironmak. Steelmak.*, 20(6), p469-475, 1993.

[8] E. Turkdogan. Fundamentals of Steelmaking, Institute of Materials, London, UK, 1996.

[9] G. Stolte. Secondary Metallurgy: Fundamentals, Processes, Applications, Verlag Stahleisen GmbH, Dusseldorf, Germany, 2002.

[10] O.N. Alzeghaibi, C.C. Sorrell, and V.H. Sahajwalla. Steel decarburization by oxide addition. Proceedings of the 2nd International Conference on Process Engineering and Advanced Materials, June 12-14, 2012 (Kuala Lumpur), the World Engineering, Science & Technology Congress (ESTCON), in press.

[11] A. Muan and S. Sōmeya, Phase relations in the system iron oxide oxide–Cr_2O_3 in air, *J. Amer. Ceram. Soc.*, 1960, 43(4), p205-209.